

Differential Proper-Motion Study of the Circumstellar Dust Shell of the Enigmatic Object, HD 179821

Brian A. Ferguson¹, Toshiya Ueta

Department of Physics and Astronomy, University of Denver, Denver, CO 80208

bferg@stsci.edu

Received July 31, 2009; accepted January 14, 2010

To Appear in ApJL

¹Current address: Space Telescope Science Institute, 3700 San Martin Dr., Baltimore,
MD 21218

ABSTRACT

HD179821 is an enigmatic evolved star that possesses characteristics of both a post-asymptotic giant branch star and a yellow hyper-giant, and there has been no evidence that unambiguously defines its nature. These two hypotheses are products of an indeterminate distance, presumed to be 1 kpc or 6 kpc. We have obtained the two-epoch Hubble Space Telescope WFPC2 data of its circumstellar shell, which shows multiple concentric arcs extending out to about $8''$. We have performed differential proper-motion measurements on distinct structures within the circumstellar shell of this mysterious star in hopes of determining the distance to the object, and thereby distinguishing the nature of this enigmatic stellar source. Upon investigation, rather than azimuthal radially symmetric expansion, we discovered a bulk motion of the circumstellar shell of $(2.41 \pm 0.43, 2.97 \pm 0.32)$ mas yr $^{-1}$. This corresponded to a translational ISM flow of $(1.28 \pm 0.95, 7.27 \pm 0.75)$ mas yr $^{-1}$ local to the star. This finding implies that the distance to HD 179821 should be rather small in order for its circumstellar shell to preserve its highly intact spherical structure in the presence of the distorting ISM flow, therefore favoring the proposition that HD 179821 is a post-AGB object.

Subject headings: circumstellar matter — ISM flow — infrared: stars — stars: AGB and post-AGB — stars: individual (HD 179821) — stars: mass loss

1. Introduction

The understanding of the nature of the evolved star HD 179821 (IRAS 19114+0002; AFGL 2343; hereafter HD 179821) is presently ambiguous. At present, there exist two plausible distance estimates for the object, hence two plausible, yet significantly different, masses and luminosities.

Metal abundances imply that HD 179821 has gone through the third dredge-up, and if so its distance would be roughly 1 kpc based on an assumed luminosity (Reddy & Hrivnak 1999). At this distance, this star is most likely a post-asymptotic giant branch (post-AGB) star with a luminosity near $1.6 \times 10^4 L_{\odot}$, implying an initial mass of $1 M_{\odot}$ (Hrivnak et al. 1989). The other competing theory, inferred from stellar expansion velocities, galactic disk models (Reddy & Hrivnak 1999), maser line observations, and an infrared (IR) excess (Jäger et al. 1994), is that HD 179821 lies at 6 kpc. At this distance, this star is most likely a yellow hyper-giant with a high luminosity near $3.1 \times 10^5 L_{\odot}$ (Hawkins et al. 1995) and an implied mass near $30 M_{\odot}$ (Schaller et al. 1992). Even the spectral type of the star is still open to scrutiny. HD 179821 was observed to be a G5Ia type star (Hrivnak et al. 1989). However, the spectroscopic surface temperature of 6800 K (which implies an F5 star) derived by Zács et al. (1996) significantly differs from what is expected for the G5Ia star (5100 K).

Despite the discrepancies, it is indisputably agreed that HD 179821 is a high luminosity object with a detached cool dust shell, which is suggestive of mass loss. This dust shell is formed during the late stages of evolution, typical for stars characterized by strong stellar winds (e.g. Waters et al. 1996). Large dusty envelopes have rarely been observed around yellow hyper-giants, but when they do, they show themselves by an infrared excess (Jäger et al. 1994). In HD 179821’s particular case, its circumstellar dust shell has been imaged in the thermal dust emission at mid-IR (Jura & Werner 1999; Ueta et al. 2001).

Five separate CO observations (Zuckerman & Dyck 1986; Likkell et al. 1987; van der Veen et al. 1993; Fong et al. 2006; Castro-Corriazo et al. 2007), and three photospheric line analyses (Zács et al. 1996; Reddy & Hrivnak 1999; Kipper 2008) suggest that HD 179821 possesses a heliocentric radial velocity of $v_r = 84.8 \pm 1.4 \text{ km s}^{-1}$, as well as a large outflow velocity, $v_{\text{exp}} = 35 \pm 2 \text{ km s}^{-1}$. The shell expansion velocity is about double the expected wind velocity of typical post-AGB type stars. Therefore the larger of the two distances is suggested, (inferring that this large shell expansion velocity suggests a more massive super-giant).

Following the discovery of the circumstellar shell of HD 179821 in the dust-scattered star light in the optical (Ueta et al. 2000) and in the near-IR, Gledhill et al. (2001) proceeded to map the shell in the OH 1667- and 1612-MHz maser lines, showing that the emission arose from a relatively thin shell whose OH dissociation characteristic is consistent with OH shell models at 6 kpc. In addition, the observed oxygen to carbon ratio of 2.6 O/C for HD 179821 is significantly large to infer that it is a low- to intermediate-mass object (Reddy & Hrivnak 1999). However, this star’s metal composition shows an overabundance of s-process elements (Zács et al. 1996; Reddy & Hrivnak 1999; Kipper 2008), which suggests the post-AGB nature of the star.

To make the matter more complicated, Reddy & Hrivnak (1999) alternatively suggested that HD 179821 is located in the Galactic disk about 4 kpc away based on the presence of spectral lines at 5780.41 and 5797.03 Å, (originating from the intervening diffuse interstellar clouds in the vicinity of the star), and the comparison between the velocity of the clouds and the radial velocity structure of the Galactic disk. Distance determination is generally one of the most difficult astronomical tasks, and this quantity remains elusive for HD 179821.

2. Differential Proper-Motion Measurements

Differential proper-motion measurements of the circumstellar shell provide a direct means for distance determination, under the assumption that (1) the rate of expansion is constant over the interval of the two measurements, (2) the expansion is understood as a radially symmetric motion, and (3) the line-of-sight expansion velocity measured by some other means is equal in magnitude to the translational expansion derived from the differential proper-motion measurements

In the past, this methodology was tested and proven successful in studying the circumstellar shells of, for example: η Car (Currie et al. 1996; Morse et al. 2001) and the Cygnus Egg Nebula (Ueta et al. 2006). Because HD 179821 was observed by the *Hubble Space Telescope* (*HST*) on 1997 July 12 (GO-6737) in the previous imaging study (Ueta et al. 2000), its shell should have expanded by anywhere from 12 to 72 milli-arcseconds over the course of roughly 10 yr at the known expansion rate of 35 ± 2 km s⁻¹ if the object is located at a distance ranging from 6 to 1 kpc, respectively. Because these expected amounts of translational expansion are detectable with the *HST*, we carried out the second epoch imaging of the object to perform the differential proper-motion measurements on 2007 July 6 (GO-10837), in order to provide another independent estimate of the distance to the object.

3. Observations and Data Reduction

For the present work we used two sets of images with the continuum F547M medium bandpass filter of the WFPC2 camera aboard the *HST*. HD 179821's shell is small enough ($\sim 8''$ diameter) to be completely observed within the Planetary Camera (PC) chip frame of WFPC2, which affords the highest resolution of the WFPC2 instrument. The first epoch

observations used for the initial condition of the differential proper-motion study were taken on 1997 July 12. The second epoch data were taken on 2007 July 6. Both sets, taken during a single orbit, include a long 30 sec exposure time.

The interval between the observations of HD 179821 provides for 10 years of stellar motion (corresponding to half a pixel at a 6 kpc distance and a constant velocity of $35 \pm 2 \text{ km s}^{-1}$, coupled with the PC pixel scale of $0''.0455 \text{ pixel}^{-1}$). To attain a clear enough image for our proper-motion measurements, we used multiple dithered exposures. Multiple exposures are needed to account for the difficulty in distinguishing between real sources and common image defects (e.g. cosmic rays). Also because these dithered images overlap, if the images are shifted a sub-pixel amount and recombined, then a sub-pixel structure can be restored (which is very important for sub-pixel level differential proper-motion analyses). The limit of this is a quarter of a pixel once the dithered images have been brought to a mosaic, which is possible with the difference-squared correlation method employed by Currie et al. (1996), Morse et al. (2001) and Ueta et al. (2006).

For data reduction, we used the standard set of WFPC2 calibration protocols as provided and defined in IRAF¹ STSDAS². Most image defects contained in the dithered images were corrected using sky mask subtraction and cosmic ray rejection tasks included in the dithered image combining task, MULTIDRIZZLE (Version 2.3: Koekemoer et al. 2002), in STSDAS. However, after this cleaning process there remained an anomaly that had to be manually corrected prior to drizzling. There was a region of slightly elevated pixel values in the middle of the PC chip, spanning roughly 140 pixels wide and extending

¹IRAF is distributed by NOAO, which is operated by the AURA, under cooperative agreement with the NSF, as a standard image reduction tool.

²Space Telescope Science Data Analysis System, Version 3.9 copyright 2003 Association of Universities for Research in Astronomy, Inc. (AURA).

for the entire 800 pixel length along the readout direction of the PC chip (i.e. across the circumstellar shell). This is caused by the bright central star being overexposed for 30 sec. As the defect was relatively constant in the affected region, we were able to estimate the amount of the pixel value elevation away from the central star and the circumstellar shell. After correcting for this anomaly, the ambient background is leveled to approximately a zero pixel value. This was performed on each of the separate images taken with the long exposure time for the epochs.

Although default distortion and rotation correction files called by MULTIDRIZZLE are accurate for a general instrumental distortion, these plate solutions called in the header of our data files were not quite good enough for our scientific goals. To measure proper motion from the two-epoch data, the images must be aligned to a sub-pixel level precision over these two epochs. In addition to the drizzling task, we performed an additional distortion correction and alignment using background stars. A total of 22 point-sources that appear in the PC chip of both sets of long exposure images were identified as references. The point-spread-function (PSF) of these reference background stars were fit by Gaussian profiles to obtain accurate positions, and then instrumental distortions were corrected with the GEOMAP and GEOTRAN tasks of STSDAS. Due to the fact that each long exposure image would have a similar distortion error as their corresponding short exposure image, we used the plate solution of the short exposure, applied it to the long, and then ran a supplemental final distortion correction on the long exposure data set. The distortion correction was carried out with an accuracy of 0.08 pixels (3.6 mas).

4. Results

After aligning two images, we carried out differential proper-motion measurements following the method elucidated and implemented previously (Currie et al. 1996;

Morse et al. 2001; Ueta et al. 2006). The nebula structures are seen via the star light scattered by dust grains in the circumstellar shell. In order to enhance the shell structure, we subtracted an azimuthally-averaged radial profile centered at the position of the star. While the general structural characteristic of the nebula is its multiple concentric shells, there are a number of distinct local structures with which we can measure the amount of differential proper motion in the shell over the 10 year interval. In total, 33 distinct positions were identified along the outer rings.

At this stage we were forced to remove any significantly saturated pixels in the image as saturated pixels throw off the matching process involved in differential proper-motion measurements. In the final drizzled images there existed two narrow diffraction spikes introduced by *HST* instrumental optics extending the length of the image. There was also a short, centered, diamond-shaped saturation spike arising from the over exposed central star. A mask was created and both effects were subsequently removed (see the top frame of Figure 1).

To determine the amount of shift, we first defined square image sections centered at each of these well-defined local structures in the epoch 1 image. The size of these image sections has to be large enough (typically ~ 10 pixels) so that the segmented structures can be uniquely identified. In the second epoch image we defined a search box that is three times larger than the image section centered at the epoch 1 position of the local structures. In the epoch 2 search box, we cut out an image section that is the same size as the epoch 1 image section and compared the two by means of cross-correlation. We did this by computing the inverse of the sum of the squares of the difference between the corresponding pixel values in the two image sections. Since this value represents the “correlation” between the two image sections, it tends to be large if the two image sections capture the same local structure (hence, the two are similar), but small if the two are different. We repeated this

operation while the epoch 2 image section was moved around inside the search box, and at the end we searched for the optimal shift that is represented by the maximum correlation. This shift is the measured shift of the local structure between the first and second epochs. This procedure was repeated for all of the 33 local structures that we selected. The middle frame of Figure 1 shows these measured shifts by arrow symbols, whose lengths correspond to the magnitudes of the shift and angles to the directions.

Surprisingly, the measured shifts of the local structures in the circumstellar shells of HD 179821 indicate that the whole nebula has exhibited a bulk motion toward the northeast direction in the plane of the sky. Under the assumption that the shell expands radially as its mass is ejected from the central star, we expect to see centrosymmetrical relative motion of sub-structures in the nebula. Still assuming that expansion should have been radially symmetric, we can search for a respective shift of the second epoch image (which is due to the bulk motion of the shell) that will recover residual shifts that are more radially symmetric—when the measured shifts of the local structures account for this induced shift of the second epoch image.

To quantitatively describe the bulk motion and to find the true differential shell expansion, we iteratively shifted the epoch 2 image and performed the differential proper-motion measurement procedure until the vectors representing residual motion of the sub-structures were pointed in the most radially outward directions. After this exercise, we were able to determine that the bulk motion of the circumstellar shell was $(2.41 \pm 0.43, 2.97 \pm 0.32)$ mas yr⁻¹. The residual shifts of the local structures are shown in the bottom frame of Figure 1. Although this search did converge, the resultant residual shift vectors do not exhibit an obvious symmetric shell expansion.

5. Discussion

5.1. Distance

The distance estimate based on the differential proper-motion measurement of the circumstellar shell relies on our ability in (1) determining the magnitudes and directions of shell expansion from the two-epoch images and (2) relating them to the known expansion velocity of the shell under the assumption of an isotropic shell expansion. Our analysis for HD 179821, however, did not conclude a symmetric shell expansion: it instead yielded residual shift vectors that show multitudes of lengths and directions. If we take the average of these resultant expansion vectors of individual shell structures to relate to 35 km s^{-1} , the distance to HD 179821 is estimated to be $3.91 \pm 3.23 \text{ kpc}$. The large error reflects a large scatter in the length of the resultant expansion vectors. Because of the large error, this result cannot address the dichotomy of the distance estimates for HD 179821.

The 33 distinct shell structures that were used to follow the shell expansion are preferentially located near the periphery of the reflection nebulosity. This is because no individual structures were identified in the central part of the shell to follow the shell motion because of the bright PSF. The most recent molecular observations of the circumstellar shells of HD 179821 have resolved a concentric structure of $\sim 2''$ radius, which is responsible for the bulk of CO and HCN emission (Castro-Corriazo et al. 2007; Quintana-Lacaci et al. 2008). Ideally, the 35 km s^{-1} expansion velocity has to be related to the expansion of this $2''$ radius molecular shell in the differential proper-motion analysis. Due to the bright central source, we were only able to follow the shell motion in regions $3''$ to $5''$ away from the central point of the object.

It is, therefore, possible that the shell expansion near the periphery of the shell, represented by the residual expansion vectors recovered in our analysis, has been taking

place at velocities lower than 35 km s^{-1} , having suffered from pile-up and slow-down of the wind material in front of the interface regions between the stellar wind and interstellar medium (ISM) as predicted numerically by, e.g., Steffen et al. (1998).

There is another possibility for the apparently slowed outer shells, although highly doubtful. Instead of being slowed by ISM interaction, it is possible that the outer shells were actually ejected during an earlier AGB phase at a lower velocity than the shells of mass most recently ejected. This scenario would imply two different spherically observed shell expansion velocities. This smaller outflow velocity would presumably be transparent in a molecular line study of radial expansion, showing two Doppler-shifted peaks about center: one for the smaller on-coming velocity of the outer shell and one for the receding velocity—neither of which are observed. Even the most recent high-resolution mapping in molecular lines bear no indication that HD 179821’s shell is expanding at anything other than a spherically consistent singular velocity. In fact the only small deviation that exists arises from the internal structure of the shell, instead of the would-be expected outer edges (Fong et al. 2006; Castro-Corrizo et al. 2007; Quintana-Lacaci et al. 2008).

With the shell expansion actually taking place at lower velocities due to the probable ISM interaction, lies the implication that the free-expansion stellar wind shell is actually of $\sim 2''$ to $3''$ radius in size and is surrounded by the region of compressed wind material in which the wind velocity is lowered. This interpretation naturally explains the fact that the resultant expansion vectors are small and appear to be oriented in seemingly random directions. Such non-radial internal motion of the shell has also been reported in molecular observations (Castro-Corrizo et al. 2007; Quintana-Lacaci et al. 2008). Thus, being that it is likely that the shell motion has been taking place at velocities lower than 35 km s^{-1} , the distance estimate obtained above (using this shell expansion value) would mean the upper limit. Regardless, using direct proper-motion analysis the distance to HD 179821 can still

be 1 or 6 kpc, and therefore, is inconclusive.

5.2. The Bulk Motion of the Shell

The detected bulk motion of the shell amounts to 0.85 pixel, about twice larger than the amount of the residual expansion vectors. There exist three obvious possibilities as the source of this bulk motion. First is proper motion of the central star, which should induce the bulk motion if the shell is co-moving with the central star. Second is motion of the ISM relative to HD 179821, which would push the shell in the direction of the ISM flow in the plane of the sky. Third is synchronized proper motion of all 22 nearby stars used to align the two epoch images. The third possibility requires all 22 stars having been moving in the same direction by the same amount over the past 10 years. We do not consider this feasible, as these stars demonstrate absolutely no differential motion between each other, after the two epoch frames have been aligned. Therefore these stars, if moving, must have a perfectly synchronized velocity in respect to their distance so as to seem all moving the exact same amount from the perspective of the Earth-based astronomer. Furthermore, no such homogeneous motion of nearby stars has been reported in, e.g., the Naval Observatory Merged Astrometric Dataset (Zacharias et al. 2004).

The central star’s proper motion is known to be $(1.13 \pm 0.85, -4.30 \pm 0.68)$ mas yr⁻¹ (van Leeuwen et al. 2007). Hence, the shell is apparently moving into the almost opposite direction in the plane of the sky. Therefore, in the frame of the central star, there is a translational ISM flow local to HD 179821 at $(1.28 \pm 0.95, 7.27 \pm 0.75)$ mas yr⁻¹, which is nearly due north in the plane of the sky. Since we have two-epoch imaging data, we should be able to confirm the *Hipparcos*-measured proper-motion of the star using our data. It turned out to be challenging because the central star was saturated even in the shortest exposure (4 sec) frames during the second-epoch observations. Nevertheless, we attempted

to measure proper motion of the star through pinpointing the location of the star by tracing the PSF spikes, (i.e. determining where the PSF spikes converge), because they should emanate from the central star.

For the epoch 1 data, in which the central star was not saturated in the shortest exposure (0.01 sec) images, we can determine if the PSF spikes would really pinpoint the position of the star. The peak centroid position of the observed star and the location where the PSF spikes cross were offset by 0.73 pix, which is larger than both of the centroiding error and the error in the PSF-spike analysis. Hence, this PSF-spike analysis would not determine the location of the central star at the astrometric accuracy that we would prefer for our purposes. However, if there is no time and on-chip-position dependent effects in the way the PSF spikes are caused by the central star the relative shift of the position of the central star determined from the PSF-spike analysis in the two epochs would represent proper motion of the star.

The PSF-spike analysis done for both epochs yielded proper motion of the star to be $(-0.08 \pm 1.58, -0.53 \pm 6.27)$ mas yr⁻¹. The large errors arose from the accuracy of linear-fitting for the PSF spikes. This means that within the error of the analysis the central star did not exhibit any appreciable amount of proper motion over the two epochs; however this error includes the *Hipparcos*-measured proper-motion of the star. (It should however be noted that the *Hipparcos*-measured proper-motion is only valid if the star is in range.)

Since the validity of this PSF-spike method to locate the position of the star has never been documented even by the WFPC2 instrument team, we have no way to access how viable our analysis is. In any event, based on the available information, we conclude that our two-epoch data of HD 179821 imply the existence of a translational ISM flow local to the object at least $(2.41 \pm 0.43, 2.97 \pm 0.32)$ mas yr⁻¹ and at most $(1.28 \pm 0.95, 7.27 \pm 0.75)$ mas yr⁻¹, dependent on the true amount of proper motion of the central star. These values

translate to $18 \pm 2 \text{ km s}^{-1}$ to $35 \pm 4 \text{ km s}^{-1}$ at 1 kpc and $109 \pm 10 \text{ km s}^{-1}$ to $210 \pm 22 \text{ km s}^{-1}$ at 6 kpc.

5.3. ISM Flow around HD 179821

The observed bulk motion of the shell around HD 179821 indicates the presence of an ISM flow local to the object irrespective of its suggested distances. Recently, similar ISM flows have been detected around other mass-losing stars based on the discrepancy between the direction of the central star’s space motion vector and the orientation of the bow shock structure at the interface between the stellar winds and the ISM inferred from far-IR images (Ueta et al. 2008, 2009a,b). HD 179821’s case does not resemble other ISM flow cases in that the shell structure of the object does not show any obvious signatures of shock interactions expected at the wind-ISM interface regions in the optical through mid-IR (Jura & Werner 1999; Ueta et al. 2000; Gledhill et al. 2001; Ueta et al. 2001; Bobrowsky et al. 2006). Other than this obvious problem, the present case is similar to the case of an asymptotic giant branch star, R Cas, for which the wind-ISM boundary appear rather circular as opposed to parabolic that is typical of a bow shock due to the inclination of the wind-ISM interface regions (22° with respect to the line of sight, Ueta et al. 2009b).

The ISM flow detected in the present analysis is only the translational component of the space motion vector of the ISM flow. The radial velocity of the star, based on the photospheric line analysis, is known to vary but is converged to the heliocentric value of 85 km s^{-1} (Zács et al. 1996; Reddy & Hrivnak 1999; Kipper 2008). Molecular observations of the shell yielded similar values (Zuckerman & Dyck 1986; Likkell et al. 1987; van der Veen et al. 1993; Fong et al. 2006; Castro-Corrido et al. 2007). Therefore, there is no evidence indicating that the shell and star are moving differently along the radial direction. Hence, there is no ISM flow local to HD 179821 in the radial direction.

Prior to this study, no evidence existed of such an ISM flow in the vicinity of HD 179821. Even the most recent high-resolution mapping in molecular lines have indicated that HD 179821’s shell is expanding fairly spherically symmetrically except for some deviation from circular symmetry seen in the internal structure of the shell (Fong et al. 2006; Castro-Corrizo et al. 2007; Quintana-Lacaci et al. 2008). Hence, if this ISM flow exists the circumstellar shell must be able to withstand the flow to maintain its more-or-less spherically symmetric characteristic. This is more so, given that the interaction between the shell of HD 179821 and the local ISM flow is viewed edge-on. Therefore, the fact that HD 179821’s shell does not show any apparent bow shock, and maintains spherical symmetry, is consistent with the expectation that the interaction between the shell and the ISM, if exists, must be benign.

The internal pressure inside the shell can be estimated as follows. Since the shell has a large physical thickness in front of the bulk of the molecular-line emitting shell (of $\sim 2''$ radius) to the edge of the reflection nebulosity (of $\sim 5''$ radius), we assume that the shell is in the energy-conserving expansion phase. Then, the internal pressure of the shell, p_{sh} , can be estimated by relating the internal energy of gas in the shell and the kinetic energy of the wind:

$$p_{\text{sh}} = \frac{\frac{1}{2}M_{\text{sh}}v_{\text{w}}^2}{2\pi R_{\text{sh}}^3}$$

where M_{sh} is the shell mass, v_{w} is the wind velocity, and R_{sh} is the radius of the shell (e.g. Lamers & Cassinelli 1999). Since $M_{\text{sh}} \geq \dot{M}t_{\text{sh}}$, where \dot{M} is the rate of mass loss ($\sim 3 \times 10^{-3} M_{\odot} \text{ yr}^{-1}$; Castro-Corrizo et al. 2007) and t_{sh} is the dynamical age of the shell (i.e. the wind crossing time, $R_{\text{sh}}/v_{\text{w}}$),

$$p_{\text{sh}} \geq \frac{\dot{M}v_{\text{w}}}{4\pi R_{\text{sh}}^2}$$

For $v_{\text{w}} = 35 \text{ km s}^{-1}$ and $R_{\text{sh}} = 5''$, $p_{\text{sh}} \geq 9.4 \times 10^{-7}$ and $2.6 \times 10^{-8} \text{ dyn cm}^{-2}$ for the shell at 1 and 6 kpc away, respectively.

On the other hand, the ISM pressure impinging on the wind-ISM interface regions, p_{ISM} , can be approximated by

$$p_{\text{ISM}} = \frac{1}{2}\rho_{\text{ISM}}v_{\text{ISM}}^2$$

where ρ_{ISM} and v_{ISM} are the mass density and velocity of the ambient ISM. The above differential proper-motion analysis yielded $v_{\text{ISM}} = 18$ and 109 km s^{-1} for the shell at 1 and 6 kpc away. Assuming the ISM number density of 1 cm^{-3} and the average ISM particle mass of 1.4 hydrogen atomic mass, $p_{\text{ISM}} = 3.9 \times 10^{-12}$ and $1.4 \times 10^{-10} \text{ dyn cm}^{-2}$ for the shell at 1 and 6 kpc, respectively. Thus, the internal pressure of the shell is much higher than the ambient ISM pressure even if the shell is 6 kpc away, and thus, the shell would be able to retain its spherical structure even with the presence of the ISM flow local to HD 179821.

Still, it remains puzzling as to why HD 179821's shell does not show any apparent signature of ram pressure stripping, which is expected from the interaction between the shell and the suspected ISM flow. The strengths of the interaction between the shell and the ISM flow are dictated principally by the *relative* velocity of the ISM in the frame of the shell (i.e. shock velocity). We have determined above that the ISM flows only in the tangential direction with respect to the local standard of rest, (as it is unlikely that an additional line-of-sight radial component of the ISM flow exists due to the symmetry of observed in the five separate CO observations (Zuckerman & Dyck 1986; Likkell et al. 1987; van der Veen et al. 1993; Fong et al. 2006; Castro-Corrido et al. 2007)). In the tangential frame of the stellar wind facing against the ISM flow, the relative ISM flow velocity amounts to 53 to 70 km s^{-1} and 144 to 245 km s^{-1} respectively at 1 and 6 kpc. It is unlikely, but if an additional radial component exists, the magnitude of the relative ISM flow will be larger; hence, these velocities are the lower limits.

This implies, therefore, that a smaller distance to HD 179821 is preferred in order for the interactions between the stellar wind and ISM to remain benign, i.e. to avoid

detection by the present and other observations. This implication is also consistent with the expectation that HD 179821 is located sufficiently closer so that there is enough ISM around the star with which it could interact. Given the Galactic latitude of the star (-5°), HD 179821 is located roughly 500 pc off the Galactic plane at 6 kpc, which would be several times the median scale-height of the Milky Way. It seems unlikely that the ISM flow at 500 pc above the Galactic plane could affect the massive circumstellar shell ($M_{\text{sh}} \sim 4 M_\odot$ at 6 kpc) in the way the present investigation has revealed.

Hence, this object appears more likely to be a post-AGB object having some high-mass star characteristics, rather than a high-mass star having a post-AGB characteristics. HD 179821 could therefore be an example of a super-AGB star (e.g. Herwig 2005), and for that, it probably warrants closer investigations into its true nature. While our analysis did not yield a decisive conclusion for the distance to this enigmatic star, HD 179821, it uncovered yet another observational trait that needs to be dealt with in understanding the true nature of the object. In any event, the distance is still the key quantity to resolve the mystery of HD 179821. VLBI astrometry may be worthwhile to make a break-through in this pursuit.

6. Summary

Based on the differential proper-motion study of the circumstellar shell structure of HD 179821 using two-epoch *HST* images taken 10 yr apart, we have found that

1. the entire shell has experienced the bulk motion at the rate of $(2.41 \pm 0.43, 2.97 \pm 0.32)$ mas yr $^{-1}$,
2. the shell's bulk motion, combined with proper motion of the star, suggests a tangential ISM flow local to HD 179821 at the rate of $(1.28 \pm 0.95, 7.27 \pm 0.75)$ mas yr $^{-1}$ at most,
3. the internal pressure of the shell is orders of magnitude higher than the ambient ISM

pressure, and hence, the shell can maintain its symmetric shape while it is being blown by the suspected ISM flow,

4. if the suggested ISM flow local to HD 179821 exists, a smaller value for the distance to the object is preferred, implying that this object is a post-AGB star with high-mass star characteristics.

This research is based on observations with the NASA/ESA *Hubble Space Telescope*, obtained at the STScI, which is operated by the AURA under NASA contract NAS 5-26555. The authors acknowledge financial support by NASA HST-GO-10837.02-A and the University of Denver’s Professional Research Opportunities for Faculty grant. The authors also thank Robert Stencel and Paul Hemenway for interesting discussions on the topic, especially on the astrometric capability of *HST*. Useful comments from the anonymous referee are also appreciated. This project’s completion is owed to the wisdom, counsel, and mentorship of Dr. Toshiya Ueta.

REFERENCES

- Bobrowsky, M., Ueta, T., & Meixner, M. 2006, in IAU Symp. 234: Planetary Nebulae in our Galaxy and Beyond, ed. M. J. Barlow & R. H. Méndez (Cambridge: CUP), 371
- Bujarrabal, V., Alcolea, J., & Planesas, P. 1992, *A&A*, 257, 701
- Castro-Carrizo, A., Quintana-Lacaci, G., Bujarrabal, V., Neri, R., & Alcolea, J. 2007, *A&A*, 465, 457
- Currie, D. G., et al. 1996, *AJ*, 112, 1115
- Fong, D., Meixner, M., Sutton, E. C., Zalucha, A., & Welch, W. J. 2006, *ApJ*, 652, 1626
- Gledhill, T. M., Chrysostomou, A., Hough, J. H., & Yates, J. A. 2001, *MNRAS*, 322, 321
- Hawkins, G. W., Skinner, C. J., Meixner, M., Jernigan, J. G., Arens, J. F., Keto, E., & Graham, J. R. 1995, *ApJ*, 452, 314
- Herwig, F. 2005, *ARA&A*, 43, 435
- Hrivnak, B. J., Kwok, S., & Volk, K. M. 1989, *ApJ*, 346, 265
- Jäger, C., Mutschke, H., Begemann, B., Dorschner, J., & Henning, T. 1994, *A&A*, 292, 641
- Jura, M., & Werner, M. W. 1999, *ApJ*, 525, L116
- Kipper, T. 2008, *Balt. Ast.*, 17, 87
- Koekemoer, A. M. 2002, *HST Dither Handbook, Version 2.0* (Baltimore: STScI)
- Lamers, H. J. G. L. M., & Cassinelli, J. P. 1999, *Introduction to Stellar Winds* (Cambridge: CUP), p.366
- Likkel, L., Morris, M., Omont, A., & Forveille, T. 1987, *A&A*, 173, L11

- Miller, G. E., & Scalo, J. M. 1979, *ApJS*, 41, 513
- Morse, J. A., Kellogg, J. R., Bally, J., Davidson, K., Ballick, B., & Ebbets, D. 2001, *ApJ*, 548, 207
- Patel M., Oudmaijer R. D., & Vink, J. S. 2008, *MNRAS*, 385, 967
- Quintana-Lacaci, G., Bujarrabal, V., & Castro-Carrizo, A. 2008, *A&A*, 488, 203
- Reddy, B. E., & Hrivnak, B. J. 1999, *AJ*, 117, 1834
- Schaller, G., Schaerer, D., Meynet, G., & Maeder, A. 1992, *A&AS*, 96, 269
- Steffen, M., Szczerba, R., & Schönberner, D. 1998, *A&A*, 337, 149
- Ueta, T., Meixner, M., & Bobrowsky, M. 2000, *ApJ*, 528, 861
- Ueta, T., Speck, A. K., Meixner, M., Dayal, A., Deutsch, L. K., Fazio, G. G., Hora, J. L., & Hoffmann, W. F. 2001, in *Post-AGB Object as a Phase of Stellar Evolution*, ed. R. Szczerba & S. K. Górný (Dordrecht: Kluwer), 339
- Ueta, T., Murakawa, K., & Meixner, M. 2006, *ApJ*, 641, 1113
- Ueta, T., et al. 2008, *PASJ*, 60, S407
- Ueta, T., et al. 2009, in *ASP Conf. Ser. AKARI - a Light to Illuminate the Misty Universe*, ed. T. Onaka, G. White, T. Nakagawa, & I. Yamamura (San Francisco: ASP), in press (arXiv:astro-ph/0905.0756)
- Ueta, T., et al. 2009, *ApJ*, submitted
- van der Veen, W. E. C. J., Trams, N. R., & Waters, L. B. F. M. 1993, *A&A*, 269, 231
- van der Veen, W. E. C. J., Waters, L. B. F. M., Trams, N. R., & Matthews, H. E. 1994, *A&A*, 285, 551

van Leeuwen, F. 2007, *A&A*, 474, 653

Waters, L. B. F. M. 1996, *A&A*, 315, L361

Zacharias, N., Monet, D. G., Levine, S. E., Urban, S. E., Gaume, R., & Wycoff, G. L.,
2004, *BAAS*, 36, 1418

Zács, L., Klochkova, V. G., Panchuk, V. E., & Spelmanis, R. 1996, *MNRAS*, 282, 1171

Zuckerman, B., & Dyck, H. M. 1986, *ApJ*, 311, 345

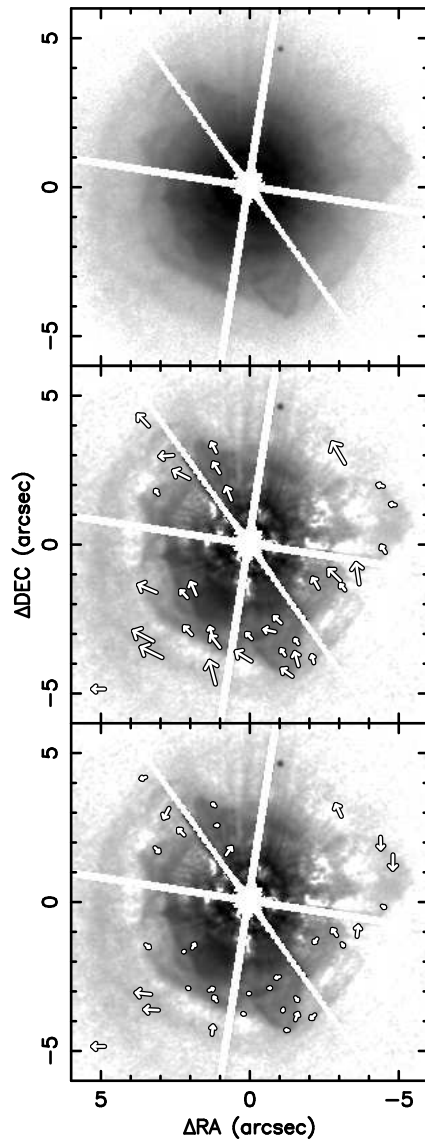


Fig. 1.— [Top] Cleaned, anomalously-corrected, masked image of HD 179821 centered at the position of the central star at the epoch 1. North is up, east to the left. Tickmarks indicate RA and DEC offsets in arcseconds. [Middle] azimuthal-average-subtracted image of HD 179821 overlaid with arrows indicating the measured differential proper-motion of the 33 local structures suggestive of the shell’s bulk motion. [Bottom] same as middle but overlaid with arrows indicating the residual differential proper-motion of the 33 local structures after the suspected bulk motion is removed. The arrow on the bottom left shows a vector corresponding to a measured one-pixel shift.